J. Astrophys. Astr. (2018) 39:48
https://doi.org/10.1007/s12036-018-9544-3

Review

The many faces of pulsars – the case of PSR B0833-45

B. RUDAK

Nicolaus Copernicus Astronomical Center, Polish Academy of Sciences, Rabiańska 8, 87-100 Toruń, Poland.
E-mail: bronek@ncac.torun.pl

MS received 16 June 2018; accepted 31 July 2018; published online 23 August 2018

Abstract. A review of observational properties of the Vela pulsar across a wide energy spectrum is given. Then current approaches to the modelling of pulsars and their wind zones are briefly presented. The challenges posed to the models by the diversity of Vela's light curves in different energy ranges are discussed.

Keywords. Pulsars—PSR B0833-45—observations—models.

1. Introduction

Almost 51 years after their discovery, pulsars are still an enigmatic phenomenon. Their key role as tools used in physics and astronomy is widely appreciated.[1] However, these tools themselves require thorough investigations in order to understand the mechanism(s) responsible for their activity. Pulsars are rapidly spinning and highly magnetized neutron stars and their electromagnetic radiation patterns are highly anisotropic. Therefore, the complete radiation characteristics of a single pulsar is impossible to determine. Moreover, ultrarelativistic charged particles (ions, electrons and positrons) escaping from pulsars in the form of magnetospheric wind can be studied only indirectly.

There are more than 2600 pulsars detected in radio pulsars (Manchester *et al.* 2005). However, pulsars are non-thermal sources, with non-coherent radiation spectra reaching X-ray and gamma-ray energy domains. Very few pulsars, however, have been detected so far at intermediate energy ranges: 1 or 2 pulsars in mid-IR, 5 in near-IR,[2] 10 in optical, 10 in near-UV and 4 in far-UV (Mignani 2017). More than 100 pulsars have been detected in soft and hard X-rays, mostly by Chandra and XMM Newton. The largest progress has been made in the gamma-ray domain (mostly by *Fermi* LAT, but also *AGILE* and earlier by SAS-2, COS B and CGRO). There are 211 gamma-ray pulsars known to date, with 115 classical pulsars and 96 millisecond pulsars. An important scientific result also came from the Imaging Atmospheric Cherenkov Telescope arrays: MAGIC, VERITAS and HESS. The Crab pulsar has its pulsed spectrum reaching now up to 1.5 TeV (Ansoldi *et al.* 2016) while the Vela pulsar has been detected between 10 GeV and 100 GeV with HESS in its mono mode (Djannati-Ataï *et al.* 2017a), and very recently around 3 TeV and 7 TeV with HESS in stereo mode (Djannati-Ataï *et al.* 2017b).

The aim of this contribution is to present the diversity of light curves across spectral frequency range observed from single pulsars as a challenge to the theories of radiation mechanism of pulsars. One of the two best-studied pulsars across wide frequency range – covering almost eighteen decades – is the Vela pulsar (the other one being the Crab pulsar). Limitations of present-day models in confrontation with Vela, as well as apparently necessary ingredients of prospect models are presented and discussed. Moreover, major models and their status are briefly presented.

2. Pulsar multiwavelength spectra and light curves

Non-thermal radiation spectra can generally be approximated by a broken power-law function and sub-exponential cutoff at high energies. In the case of Crab pulsar, the high-energy cutoff has the form of the steep power-law tail, reaching 1.5 TeV.

[1] David Finley (NRAO) aptly called them 'Pulsars: The Universe's Gift to Physics'.

[2] The IR observations could not be carried out in phased modes, hence the measured fluxes are unpulsed.

Non-thermal light curves consist of rather narrow pulses, with high pulsed fraction, and are energy dependent in most cases.

Thermal spectral components (in soft X-rays) are fitted either by blackbody or by strongly magnetized atmospheric models (H, He or Fe). The soft X-ray light curves show smooth pulsations, with low-pulsed fraction.

A good example of a pulsar containing all such radiation properties is for instance, Geminga (see Mori *et al.* 2014).

2.1 *The Vela pulsar* (*PSR B0833-45*)

The non-coherent radiation from Vela extends from (at least) near-IR (Zyuzin *et al.* 2013) in the low-frequency end of the spectrum, to optical (Gouiffes 1998), near-UV and far-UV (Romani *et al.* 2005), to soft (Pavlov *et al.* 2001) and hard X-rays (Harding *et al.* 2002), to gamma-rays (Abdo *et al.* 2010; Djannati-Ataï *et al.* 2017a), reaching the VHE range at 3 TeV and 7 TeV (Djannati-Ataï *et al.* 2017b). The subset of Vela's light curves is shown in Fig. 1 and Fig. 2, and its energy flux density is shown in Fig. 3.

The shapes and phases of the pulses observed from Vela impose questions which are difficult to answer:

- What is the origin of radiation at different frequency ranges? The overall shape of the flux density spectrum does not look too complex. Therefore, it is tempting to look for a single radiative process as responsible for the entire spectrum.
- Why two main peaks in optical are not aligned with two main peaks in gamma-rays (indicated with two vertical blue lines)?
- Why their shapes are so different from the gamma-ray pulse shapes?
- What is the origin of a narrow peak at phase 0.0 present in optical, UV and hard X-rays (note another narrow peak in hard X-rays at phase 0.85), aligned with the radio pulse (vertical red line)?
- Why an analogous peak is not present in gamma-rays (the bottom panel)?

We are not aware of any attempts to address these questions within the existing (but otherwise elaborated and detailed in many aspects) models of pulsar mechanism.[3]

[3]We note, however, that the peak-to-peak separation of 0.25 in optical had been reproduced with simple estimates within the outer-gap scenario (Cheng *et al.* 1986).

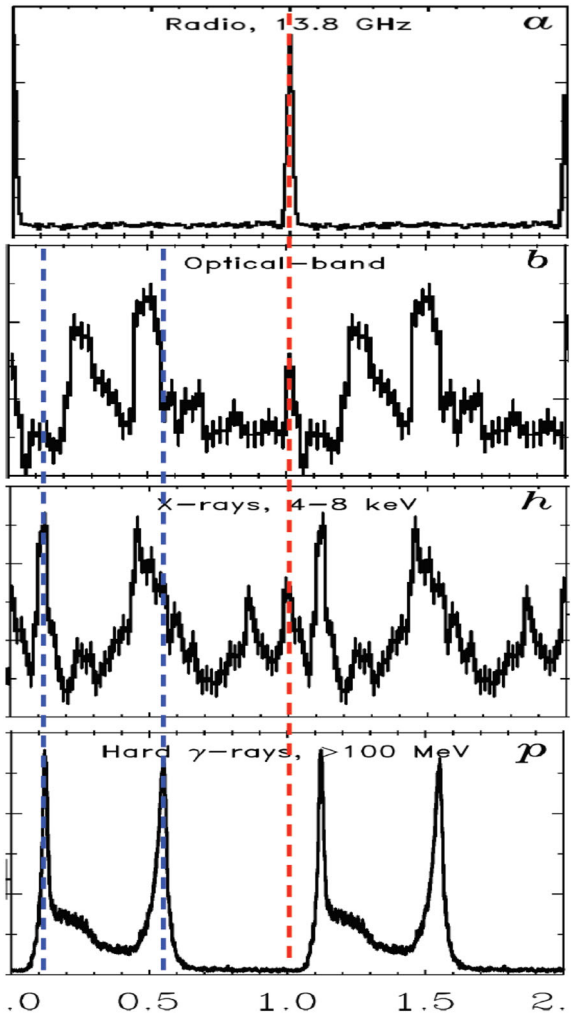

Figure 1. The many faces of the Vela pulsar: its light curves in radio, optical, hard X-rays and gamma rays (based on Fig. 4 of Kuiper & Hermsen (2015)).

3. A brief account of present-day pulsar models

3.1 *The co-rotating magnetosphere models*

The co-rotating magnetospheres in low-density, charge-separation limit, are so far the most popular models using different types of accelerating gaps. Three major types of magnetospheric accelerators (coming in many flavours) have been proposed:

- inner gap,
- outer gap,
- TPC-slot gap.

Their popularity evolves with time, as more and more high-quality observations in different energy domains become available (the inner gap models are not

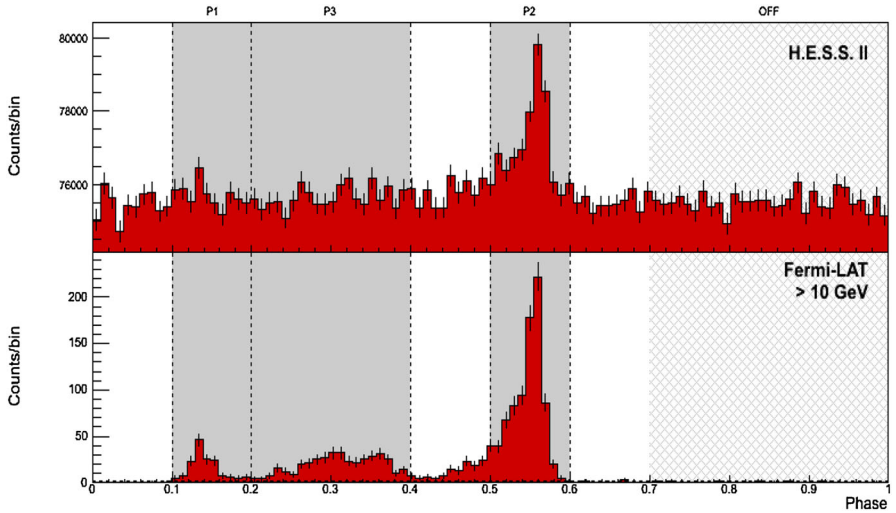

Figure 2. The Vela phasogram above 10 GeV according to HESS II monodata (*top*) and *Fermi*-LAT data (*bottom*) (Djannati-Ataï *et al.* 2017a).

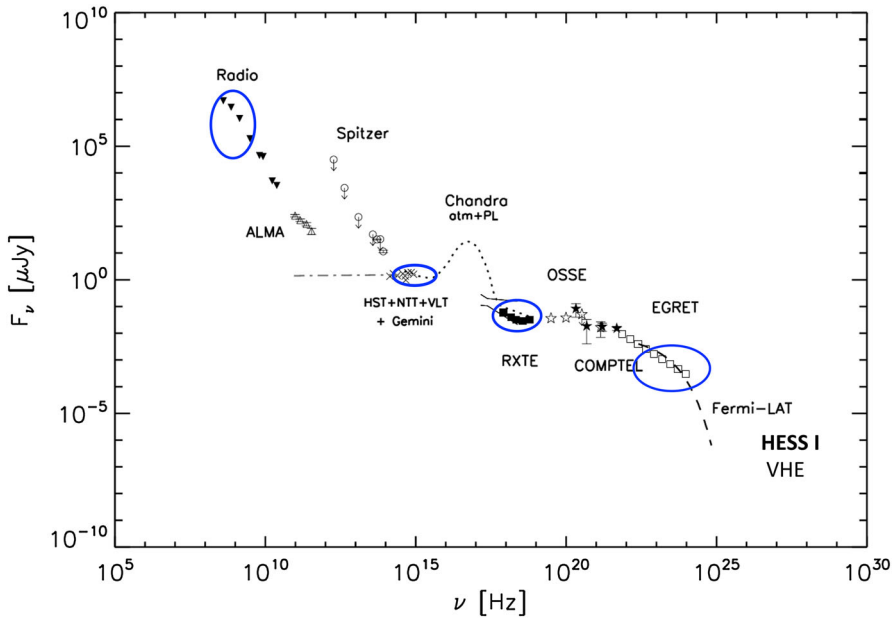

Figure 3. The flux density of Vela pulsar. Encircled in blue are the (phase-averaged) data points in four energy bands corresponding to four panels of Fig. 1 with the light curves. This figure is based on Fig. 2 of Mignani *et al.* (2017).

preferred any more for young or middle-aged classical pulsars, and even for millisecond pulsars).

The models require simultaneous solution in the magnetosphere of non-vacuum Poisson equation, Boltzmann equation for pairs, and radiative transfer (e.g. Hirotani 2015). The boundary conditions are assumed and hence many flavours of each type of model are possible. Global current closure problem is not addressed in those models.

Despite many elaborations in the numerical 3D simulations, the results are not fully satisfactory, either with respect to the spectra or with respect to the light curves, or both.

The three-dimensional slot gap model of the spectral energy distribution by Harding and Kalapotharakos (2015) is one of latest and detailed attempts to model the radiation spectrum of Vela pulsar. However, their slot gap follows the magnetic field lines of different shapes (see the next subsection) than the Deutsch solution used in the low-density magnetosphere; moreover, it extends beyond the light-cylinder radius.

3.2 *Global electrodynamics with the plasma*

The aim of this approach is to formulate self-consistent electrodynamics, with global current closure.

This became possible with the seminal paper of Contopoulos *et al.* (1999) presenting a method to solve the force-free axisymmetric magnetosphere numerically. Further, an important step came with the numerical solution of the force-free magnetosphere in an oblique rotator case (Spitkovsky 2006). The existence of the current sheet was also confirmed there.

The starting point in this ambitious approach were force-free electrodynamics (FFE) models of magnetospheres and winds. The entire dissipation of the rotational energy is, therefore, occuring outside the magnetosphere, beyond the light cylinder (i.e. in the winds).

The next step is the modelling of dissipative magnetospheres and winds (outflow of dense plasma and Poynting flux). The simplest approach is to use the MHD approximation with some macroscopic conductivity – a purely phenomenological, free parameter.

Modelling microscopic conductivity has been carried out with particle-in-cell (PiC) simulations, including $e^{\pm}$-pair creation and acceleration (due to magnetic reconnections).

Strong synchrotron emission is then possible in the current sheet and in the separatrix sheets inside the light cylinder (Lyubarsky 1990; Spitkovsky 2006; Cerutti *et al.* 2016; Philippov & Spitkovsky 2018).

For an inclined rotator the current sheet becomes corrugated, and the striped wind forms, leading in turn to pulsed emission. An example of such an emission is presented in Fig. 4, where the Crab pulsar data from CGRO COMPTEL, *Fermi*-LAT and MAGIC are fitted with the current-sheet model of Mochol and Pétri (2015) and Mochol (2017). The main part of the presented model SED (between 10 MeV and ∼100 GeV) is due to Doppler-boosted synchrotron emission within the current sheet. Below 10 MeV, another component (not discused in the framework of the current sheet model) apparently takes over and dominates the entire SED of the Crab pulsar. In the case of the Vela pulsar, however, single synchrotron component originating in the current sheet is sufficient to reproduce the phase-averaged SED, according to Mochol and Pétri (2015). No light curves are included in the model, though. Within the presented framework, the current sheet model is not expected to reproduce the diversity of the light curves in Fig. 1 and Fig. 2 as well as their mutual phase shifts. In particular, the current sheet model cannot reproduce the phase lag of ∼0.1 of the leading gamma-ray peak behind the radio peak (see panels (a) and (p) connected by the dashed vertical line in Fig. 1, and Abdo *et al.* (2013) for the

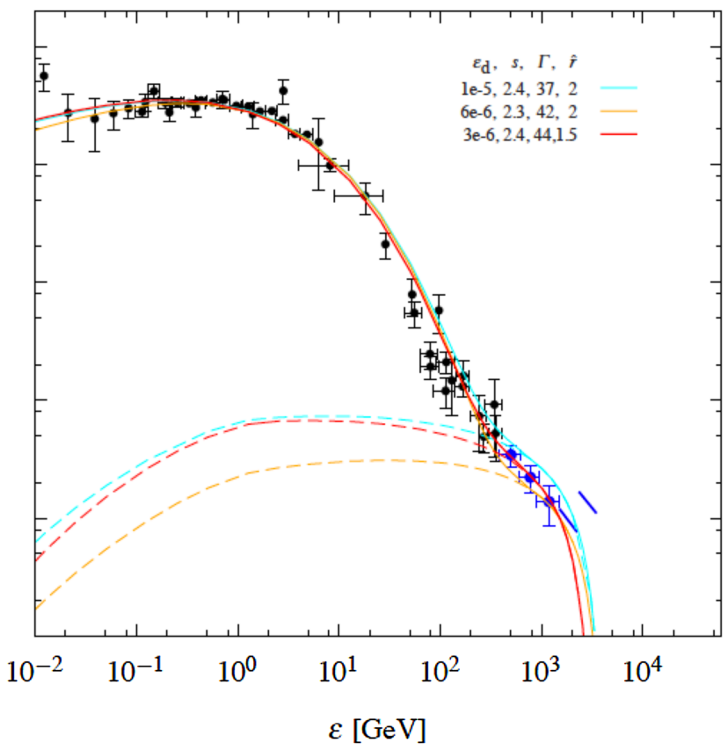

Figure 4. The high energy (below 100 GeV) and VHE (above 100 GeV) spectral energy distribution for the Crab pulsar in the current sheet model of Mochol and Pétri (2015) and Mochol (2017). The model reproduces the shape and magnitude of the VHE spectral component reaching 1.5 TeV (Ansoldi *et al.* 2016).

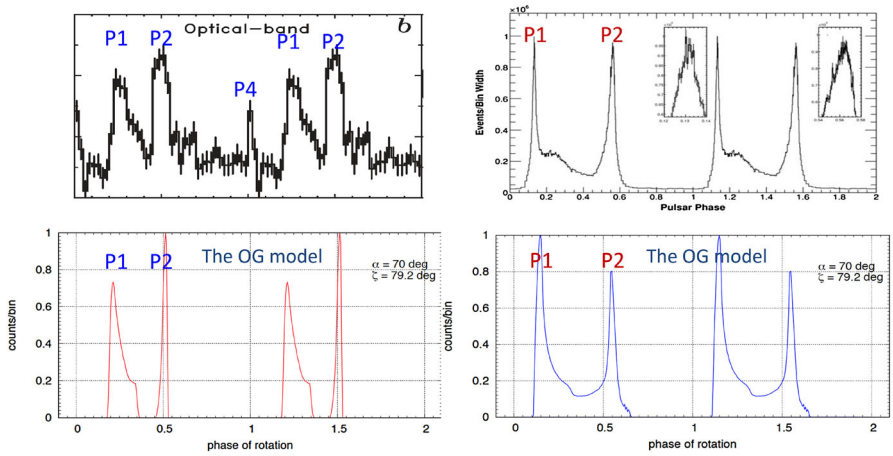

Figure 5. *Top*: The P1 and P2 pulses from Vela in optical (Gouiffes 1998) and gamma rays (Abdo *et al.* 2010). *Bottom*: Their reconstruction in the uniform-emissivity version of the OG model, obtained for inclination angle $\alpha = 70°$ and viewing angle $\zeta = 79°$ (Rudak & Dyks 2017).

gamma-radio phase lags in other pulsars); its capabilities in this respect are limited to just a few pulsars with gamma-ray and radio light curves showing a mirror symmetry with respect to the phase 0.5 (see Fig. 8 of Pétri 2011).

Therefore, the case of the Vela pulsar light curves seems to be particularly difficult to understand within the scenario of the current sheet. Some contribution to the pulsed radiation coming from the inner magnetospere and/or the separatrix seems to be unavoidable. The presence of magnetospheric gaps (as addressed in section 3.1) is also necessary to supply the electron–positron plasma. The gaps also impose the boundary conditions on the force-free zone of the magnetosphere.

4. The arguments for the presence and co-existence of outer gaps and inner gaps in the Vela pulsar

The semi-phenomenological model capable of reproducing (at least qualitatively) the observed properties of Vela radiation has been proposed recently (Rudak & Dyks 2017). It is based on the 3D outer gap model. It reproduces two main pulses in gamma-rays (as due to curvature emission) and optical (as due to synchrotron emission), in terms of their phases and shapes (see Fig. 5). The model contains an additional inner gap; this is essentially possible, since both types of gaps occupy different open magnetic field lines.

The idea of coexisting gaps is not new and was used in many papers (by the tacit assumption), like Watters *et al.* (2009) or Venter *et al.* (2009) in the context of confronting the outer-gap models and slot-gap models with the Fermi *LAT* gamma-ray pulsars. Polar gaps exist in these models and are assumed to be responsible for a narrow radio pulse (whenever observed) in the gamma-ray pulsars.

On the theoretical side, this concept has attracted some interest in the context of studying the properties of force-free magnetospheres (e.g. numerical simulations of the coexisting gaps by Yuki & Shibata (2012) and the analytical model by Petrova (2013).

Three different inverse Compton scattering processes involving the proposed gaps are considered (see Fig. 6):

(1) outer-gap primary electrons colliding with soft (i.e. optical-infrared) photons originating from the adjacent synchrotron (SR) layer,
(2) inner-gap pairs interacting with optical-infrared photons originating from the SR layer,
(3) inner-gap pairs interacting with thermal X-ray photons from the neutron star surface.

These processes lead to the formation of

(1) spectral component in the VHE range (the prediction),
(2) core-like pulse detected in optical as well as in UV at the phase of the radio core pulse,
(3) core-like pulse detected in hard X-rays at the phase of the radio core pulse.

The numerical calculations show the formation of core-like pulses in optical, UV and in hard X-rays, aligned in phase with the core-like radio pulse, as observed. In very high energy domain, a new spectral component emerges, with the light curve shown in Fig. 7. Its predicted flux is within reach by the future CTA observatory (see Rudak & Dyks (2017) for the results).

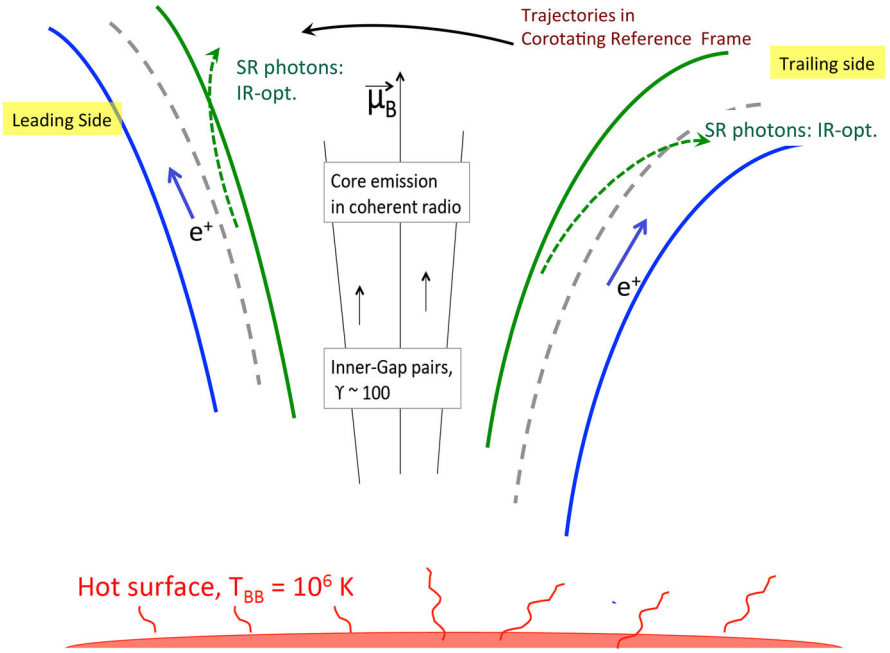

Figure 6. Cartoon of coexisting gaps (inner and outer) and the hot NS surface in the model of Vela (Rudak & Dyks 2017). Screened region: secondary pairs with $\gamma_{\pm} \sim 100$–1000 emit synchrotron photons from hard X-rays to optical to mid-IR. The SR photon trajectories (dashed green) are shown in the co-rotating reference frame (CF) Accelerating gap region: primary electrons with $\gamma_e > 10^7$ (blue arrow trajectories in CF) emit curvature photons. They also upscatter some SR photons due to colliding trajectories, preferentially on the trailing side of the open magnetic field-line volume. The inner gap region is a postulated site of pair creation with $\gamma_{\pm} \sim 100$–1000; these pairs are thought to be responsible for coherent radio emission forming the 'core' pulse at phase 0 in Fig. 1. The photon field of thermal X-rays due to initial cooling from the NS surface is a target for the pairs in Compton upscattering, leading to the formation of P4 in optical, UV and X-rays (see Fig. 1).

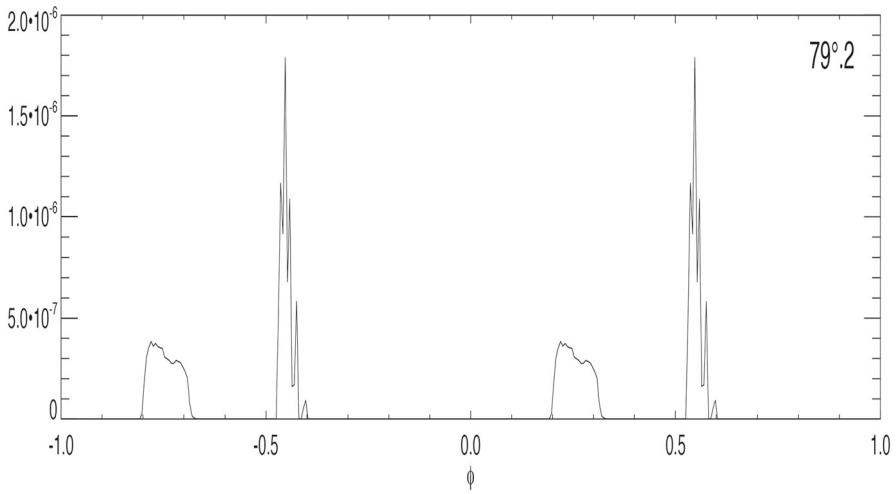

Figure 7. The light curve at 3 TeV of the inverse Compton scattering spectral component resulting from the model depicted in Fig. 6. It consists of two pulses of different shapes and amplitude. The leading and trailing pulses are located at the phase interval of 0.2–0.3 and 0.5–0.6, respectively.

5. Summary and conclusions

The outer gap model with an adjacent layer of the $e^{\pm}$-pair formation reproduces simultaneously two main pulses in gamma-rays and in optical, in terms of their phases and shapes, as observed in the Vela pulsar.

Introducing an inner gap with $e^{\pm}$ pairs as coexisting with the outer gap leads to the formation of core-like pulses in optical, UV and hard X-rays, in phase with the core-like radio pulse, as observed in the Vela pulsar.

A distinct spectral component is formed in the VHE range. Its light curve consists of two pulses at phases

0.2 and 0.6, and its expected flux at 3 TeV for the Vela pulsar should be of interest to CTA South (for >50 h).

Multiwavelength properties of the Vela pulsar should be taken into account when developing the models relying on the wind and current-sheet activity only.

Acknowledgement

The author acknowledges financial support by the National Science Centre, Grant DEC- 2011/02/A/ST9/00256.

References

Abdo A. A., Ackermann M., Ajello M., Allafort A. *et al.* 2010, ApJ, 713, 154
Ansoldi S. *et al.* 2016, Astron. Astrophys. 585, A133
Cheng K. S., Ho C., Ruderman M. 1986, ApJ, 300, 522
Cerutti B., Philippov A. A., Spitkovsky A. 2016, MNRAS, 463, 89
Contopoulos I., Kazanas D., Fendt C. 1999, ApJ, 511, 351
Deutsch A. J. 1955, AnAp, 18, 1
Djannati-Ataï A. *et al.* 2017a, 6th International Symposium on High Energy Gamma-Ray Astronomy, vol. 1792 of American Institute of Physics Conference Series, 040028
Djannati-Ataï A. *et al.* 2017b, 29th Texas Symposium on Relativistic Astrophysics
Gouiffes C. 1998, Proceedings of the International Conference on Neutron Stars and Pulsars, Tokyo (Japan) 1997, edited by Shibazaki N. *et al*., Universal Academy Press, Tokyo, Japan (Frontiers Science Series) 24, 363
Harding A. K. *et al.* 2002, ApJ, 576, 376
Harding A. K., Kalapotharakos C. 2015, ApJ, 811, 63
Hirotani K. 2015, ApJ, 798, 40
Kalapotharakos C., Kazanas D., Harding A. K., Contopoulos I. 2012, ApJ, 749, 2
Kuiper L., Hermsen W. 2015, MNRAS, 449, 3827
Lyubarsky Y. E. 1990, Sov. Astron. Lett., 16, 16
Manchester R. N., Hobbs G. B., Teoh A., Hobbs M. 2005, Astron. J., 129, 1993, astro-ph/0412641
Mignani R. P. 2017, Contribution to IV Workshop sull'astronomia millimetrica in Italia
Mignani R. P., Paladino R., Rudak B., Zajczyk A. *et al.* 2017, ApJ, 851L, 10
Mochol I., Pétri J. 2015, MNRAS, 449, L51
Mochol I. 2017, ASSL, 446, 135
Mori K., Gotthelf E. V., Dufour F., Kaspi V. M. *et al.* 2014, ApJ, 793, 88
Pavlov G. G., Zavlin V. E., Sanwal D., Burwitz V. *et al.* 2001, ApJ, 552, L129
Pétri J. 2011, MNRAS, 412, 1870
Petrova S. A. 2013, ApJ, 764, 129
Philippov A. A., Spitkovsky A. 2018, ApJ, 855, 94
Romani R. W., Kargaltsev O., Pavlov G. G. 2005, ApJ, 627, 383
Rudak B., Dyks J. 2017, Proceedings of 35th ICRC, Busan (Korea) 2017, journal-ref: PoS(ICRC2017)680
Spitkovsky A. 2006, ApJ, 648, L51
Spitkovsky A. 2016, ApJ, 648, 51
Venter C., Harding A. K., Guillemot L. 2009, ApJ, 707, 800
Watters K. P., Romani R. W., Weltevrede P., Johnston S. 2009, ApJ, 695, 1289
Yuki S., Shibata S. 2012, PASJ, 64, 4
Zyuzin D., Shibanov Y., Danilenko A., Mennickent R. E., Zharikov S. 2013, ApJ, 775, 101